

Fig. 8. Measured output amplitude and phase linearity for the prototype AMO system with DPWM. Each curve corresponds to a different combination of discrete pulse widths for the two outphased PAs. The ideal curves for the output amplitude are shown in black.

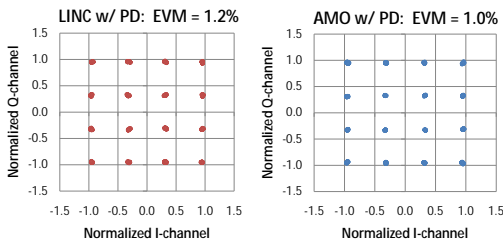


Fig. 9. Measured EVM of 50-ksym/s 16-QAM with 6.5-dB PAPR after predistortion.

the same discrete pulse width and are completely out of phase, as can be seen in Fig. 8. Thus it is important that the discrete levels and combinations are chosen to achieve sufficient amplitude dynamic range while maximizing the overall efficiency. A lookup table constructed from the data in Fig. 8 is used to correct for the static nonlinearity.

To demonstrate the linearity of the system, we tested the prototype with a 50-ksym/s 16-QAM signal with a PAPR of 6.5 dB and a carrier frequency of 48 MHz. The digital baseband data generation and associated signal processing were performed in MATLAB and uploaded into the internal memory of arbitrary function generators. The baseband phase data for each PA was upconverted to 48 MHz with an Agilent vector signal generator, and the system output was fed into an HP 89400 vector signal analyzer for spectrum and error vector magnitude (EVM) analysis. Fig. 9 shows the measured demodulated 16-QAM constellation of the prototype for both the standard LINC case and for the AMO-DPWM system after predistortion. After predistortion, the EVM is reduced to 1.0%. Fig. 10 shows the measured output spectrum for the 50-

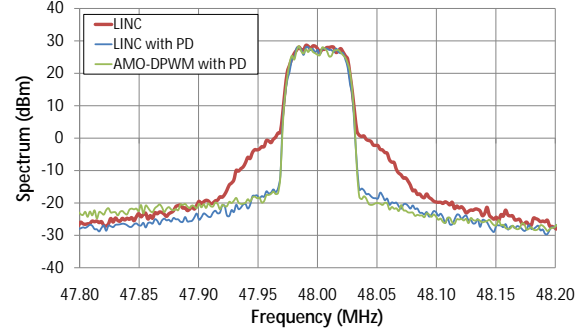


Fig. 10. Measured transmit spectrum of the 16-QAM signals.

ksym/s 16-QAM transmission. For the 50-ksym/s 16-QAM signal, the AMO system improves the overall efficiency from 17.1% to 36.5% compared to the standard LINC system, an efficiency improvement of more than 2x.

VI. CONCLUSIONS

The AMO transmitter using class-E PAs with DPWM was proposed to not only greatly increase transmitter efficiency but also enable wideband RF transmission. The DPWM technique was described as a method to provide an efficient coarse output envelope control, with outphasing providing the remaining fine envelope control. Finally, we demonstrate a 4-level AMO transmitter at 48 MHz which improves the overall efficiency from 17.1% to 36.5% for a 50-ksym/s 16-QAM signal with a PAPR of 6.5 dB.

REFERENCES

- [1] F. H. Raab, "Power amplifiers and transmitters for RF and microwave," *IEEE Trans. Microwave Theory Tech.*, vol. 50, no. 3, pp. 814–826, Mar. 2002.
- [2] H. Chireix, "High-power outphasing modulation," *Proc. of the IRE*, vol. 23, pp. 1370–1392, 1935.
- [3] D. C. Cox, "Linear amplification with nonlinear components," *IEEE Trans. Commun.*, pp. 1942–1945, Dec. 1974.
- [4] S. Moloudi, K. Takinami, M. Youssef, M. Mikhemar, and A. Abidi, "An outphasing power amplifier for a software-defined radio transmitter," in *ISSCC Dig. Tech. Papers*, 2008, pp. 568–569.
- [5] R. Beltran, F. H. Raab, and A. Velazquez, "HF outphasing transmitter using class-E power amplifiers," in *Proc. IEEE Int'l Microwave Symp.*, 2009, pp. 757–760.
- [6] J. Keyser, R. Uang, Y. Sugiyama, M. Iwamoto, I. Galton, and P. Asbeck, "Digital generation of RF pulsewidth modulated microwave signals using delta-sigma modulation," in *Proc. IEEE Int'l Microwave Symp.*, 2002, pp. 397–400.
- [7] J. S. Walling, S. S. Taylor, and D. J. Allstot, "A class-G supply-modulator and class-E PA in 130 nm CMOS," *IEEE J. Solid-State Circuits*, vol. 44, no. 9, pp. 2339–2347, Sept. 2009.
- [8] S. Chung, P. A. Godoy, T. W. Barton, E. W. Huang, D. J. Perreault, and J. L. Dawson, "Asymmetric multilevel outphasing architecture for multistandard transmitters," in *Proc. IEEE RFIC Symp.*, 2009, pp. 237–240.
- [9] F. H. Raab, "Idealized operation of the Class E tuned power amplifier," *IEEE Trans. Circuits Syst. II*, vol. CAS-24, no. 12, pp. 725–735, Dec. 1977.
- [10] P. Godoy, D. J. Perreault, and J. L. Dawson, "Outphasing energy recovery amplifier with resistance compression for improved efficiency," *IEEE Trans. Microwave Theory Tech.*, Dec. 2009.